28 May 2024

ALMA MATER STUDIORUM
UNIVERSITÀ DI BOLOGNA

ARCHIVIO ISTITUZIONALE
DELLA RICERCA

Alma Mater Studiorum Università di Bologna
Archivio istituzionale della ricerca

Probing the effect of β-triketonates in visible and NIR emitting lanthanoid complexes

This is the final peer-reviewed author's accepted manuscript (postprint) of the following publication:

Published Version:
Probing the effect of β-triketonates in visible and NIR emitting lanthanoid complexes / Abad Galán, Laura; Reid, Brodie L.; Stagni, Stefano; Sobolev, Alexandre N.; Skelton, Brian W.; Moore, Evan G.; Hanan, Garry S.; Zysman-Colman, Eli*; Ogden, Mark I.; Massi, Massimiliano. - In: DALTON TRANSACTIONS. - ISSN 1477-9226. - STAMPA. - 47:24(2018), pp. 7956-7964. [10.1039/c8dt00945g]

This version is available at: https://hdl.handle.net/11585/644973 since: 2019-01-21

Published:

DOI: http://doi.org/10.1039/c8dt00945g

Terms of use:

Some rights reserved. The terms and conditions for the reuse of this version of the manuscript are specified in the publishing policy. For all terms of use and more information see the publisher's website.

(Article begins on next page)

This item was downloaded from IRIS Università di Bologna (https://cris.unibo.it/).
When citing, please refer to the published version.

This is the final accepted manuscript of:

Probing the effect of β-triketonates in visible and NIR emitting lanthanoid complexes

Laura Abad Galán, Brodie L. Reid, Stefano Stagni, Alexandre N. Sobolev, Brian W. Skelton, Evan G. Moore, Garry S. Hanan, Eli Zysman-Colman, Mark I. Ogden, Massimiliano Massi. *Dalton Transactions* **2018** *47*, 7956-7964
DOI: 10.1039/C8DT00945G

Publication Date (Web): May 17, 2018
Available at: https://pubs.rsc.org/en/content/articlepdf/2018/dt/c8dt00945g

Copyright © 2018 Royal Society of Chemistry

Probing the effect of β-triketonates in visible and NIR emitting lanthanoid complexes

Laura Abad Galán,[a,b] Brodie L. Reid,[a] Stefano Stagni,[b] Alexandre N. Sobolev,[c] Brian W. Skelton,[c] Evan G. Moore,[d] Garry S. Hanan,[e] Eli Zysman-Colman,[*f] Mark I. Ogden,[*a] and Massimiliano Massi[*a]

An isomorphous series of lanthanoid complexes containing tribenzoylmethanide (**tbm**) and 1,10-phenanthroline (**phen**) ligands has been synthesised and structurally characterised. These complexes, formulated as [Ln(**phen**)(**tbm**)$_3$] (Ln = Eu^{3+}, Er^{3+} and Yb^{3+}), were compared with analogous dibenzoylmethanide (**dbm**) [Ln(**phen**)(**dbm**)$_3$] complexes to investigate the effect of changing β-diketonate to β-triketonate ligands on the photophysical properties of the complex. The photophysical properties for the Eu^{3+} complexes were similar for both systems, whereas a modest enhancement was observed for Yb^{3+} and Er^{3+} moving from the **dbm** to the **tbm** complexes. A detailed study of the NIR photophysical properites was achieved by adapting the integrating sphere method for the calculation of overal quantum yields in the solid state.

Introduction

Luminescent trivalent lanthanoid complexes present characteristic intraconfigurational *f-f* transitions that result in line-like emission profiles and relatively long-lived excited state lifetime decays. Depending on the specific lanthanoid ion, the emission ranges from the visible to the near-infrared (NIR) spectral region. Particular interest in emission from lanthanoid complexes has arisen due to their wide range of applications from bioimaging to night vision technologies and telecommunication signalling.[1–5] However, since *f-f* transitions are parity- and often spin-forbidden, the use of antenna chromophores is required to enhance their luminescence efficiency. In order to have an effective sensitisation and prevent back energy transfer, the lowest triplet state of the antenna needs to lie at ~3,500 cm^{-1} above the emitting excited states of the lanthanoid.[6,7] Furthermore, high energy oscillators in close proximity to the metal centre, such as O-H, N-H and C-H, are able to quench the NIR and visible lanthanoid emitting states.[8] Therefore, extra effort in the design of the lanthanoid emitters has been made in order to favour the energy transfer from the antenna and minimise non-radiative decay pathways.[9–11] β-Diketonates have been extensively studied because they strongly bind trivalent lanthanoid ions while being able to sensitise their emission according to their chemical nature. A variety of different structural motifs incorporating β-diketonates can be found in the literature over the last couple of decades.[12–16] Various strategies have been followed to improve the luminescence properties of the NIR lanthanoid complexes by means of reducing non-radiative decay pathways. These include the perfluorination and deuteration of the β-diketones, extending their π conjugated systems and, in particular, the use of an ancillary ligand in order to replace coordinating solvent molecules.[14,15,17–19]

In our previous work, we have reported unusual and improved photophysics for the NIR emitters based on the use of β-triketonates as sensitisers. This characteristic motivated us to further investigate β-triketonates as sensitisers for lanthanoid luminescence.

β-Triketonates are of interest because the additional ketone O-donor atom permits the formation of multinuclear metal assemblies. Our previous studies[20–22] with tribenzoylmethanide (**tbm**) and tris(4-methylbenzoyl)methanide (**mtbm**) ligands showed that tetranuclear assemblies formed upon reaction of these ligands with various lanthanoid salts and in the presence of alkali

[a] *Department of Chemistry, and Curtin Institute for Functional Molecules and Interfaces, Curtin University, Kent Street, Bentley 6102 WA, Australia.*
[b] *Department of Industrial Chemistry "Toso Montanari" – University of Bologna, viale del Risorgimento 4, Bologna 40136, Italy.*
[c] *School of Molecular Sciences, M310, University of Western Australia, Crawley 6009 WA, Australia.*
[d] *School of Chemistry and Molecular Biosciences, University of Queensland, St Lucia 4072 QLD, Australia.*
[e] *Department of Chemistry, D-600 Université de Montréal, 2900 Edouard-Montpetit Montréal, Quebec, Canada.*
[f] *Organic Semiconductor Centre, EaStCHEM School of Chemistry, University of St. Andrews, St. Andrews, Fife, KY16 9ST, United Kingdom*
*E-mail: m.massi@curtin.edu.au; m.ogden@curtin.edu.au; eli.zysman-colman@st-andrews.ac.uk

† Electronic Supplementary Information (ESI) available: The Supporting information contains details of X-ray diffraction studies of [Ho(**tbm**)$_3$(EtOH)(H_2O)]·EtOH, shape analysis plots, first coordination sphere overlay between [Ln(**phen**)(**tbm**)$_3$] and [Ln(**phen**)(**dbm**)$_3$], [Eu(**phen**)(**tbm**)$_3$] emission studies in EtOH, normalised excitation spectra and excited lifetime decays for [Ln(**phen**)(**tbm**)$_3$] and [Ln(**phen**)(**dbm**)$_3$] and Er^{3+} complexes emission profiles in the solid state.

metal hydroxides. When the alkali metal (Ae) was Na^+, K^+ or Rb^+ cations, discrete tetranuclear assemblies $[Ln(Ae{\cdot}HOEt)(\mathbf{tbm})_4]_2$ formed. By contrast, with Cs^+, polymeric structures of the form $[(LnCs(\mathbf{tbm})_4)_2]_n$ or $[(LnCs(\mathbf{mtbm})_4)_2]_n$ (Ln = Eu^{3+}, Er^{3+}, Yb^{3+}) were isolated.

For both types of structures, remarkably long-lived lifetimes and improved quantum yields were achieved for NIR-emitting assemblies of Er^{3+} and Yb^{3+} in comparison to complexes containing β–diketonate ligands, even in cases where the diketone had been perfluorinated or deuterated. While the main reason for this improvement may be the reduction of multiphonon relaxation pathways caused by the removal of the proton on the α-C atom, other structural effects should be taken into account. In order to do so, a system with similar coordination spheres for both ligands, β-diketonate and β-triketonate, must be found. Given the flexible geometries of lanthanoid complexes, finding systems with negligible variation of the coordination spheres is not an easy task. Moreover, analogous β-diketonate-based Ln_2Ae_2 assemblies do not exist and so an alternative needs to be proposed.

In the present work, we compare a new family of monomeric β-triketonate complexes containing **tbm** and **phen** ligands ($[Ln(\mathbf{phen})(\mathbf{tbm})_3]$, Ln = Eu^{3+}, Er^{3+} and Yb^{3+}), with the analogous previously reported dibenzoylmethanide (**dbm**) $[Ln(\mathbf{phen})(\mathbf{dbm})_3]$ complexes. Fortunately, in this case, similarities in composition and structure between the β-diketonate and β-triketonate complexes were found, making it possible to compare more closely their photophysical properties. The monomeric complexes have been studied by absorption and emission spectroscopies. Furthermore, an adapted method was followed for the calculation of the overall quantum yields for the NIR emitters, providing full characterisation of their photophysical properties. The results show only a small enhancement for the NIR β-triketonate-based complexes, suggesting that structural and composition factors must be considered to explain the remarkable properties of the previously reported tetranuclear complexes.

Experimental

General procedures

All reagents and solvents were purchased from chemical suppliers and used as received without further purification. The ligand precursor 2-benzoyl-1,3-diphenyl-1,3-propandione (tribenzoylmethane - **tbm**H) was prepared as previously reported.[20] Hydrated $LnCl_3$ (Ln = Eu^{3+}, Er^{3+} and Yb^{3+}) were prepared following a previously reported method by the reaction of the corresponding Ln_2O_3 with hydrochloric acid.[23] Infrared spectra (IR) were recorded on solid state samples using an Attenuated Total Reflectance (ATR) Perkin Elmer Spectrum 100 FT-IR. IR spectra were recorded from 4000 to 650 cm^{-1}; the intensities of the IR bands are reported as strong (s), medium (m), or weak (w), with broad (br) bands also specified. Melting points were determined using a BI Barnsted Electrothermal 9100 apparatus. Elemental analyses were obtained at Curtin University (Australia), or the Université de Montréal (Canada). Nuclear magnetic resonance (^1H and ^{13}C NMR) spectra were recorded using a Bruker Avance 400 spectrometer (400.1 MHz for ^1H; 100 MHz for ^{13}C) at room temperature. The data were acquired and processed by the Bruker TopSpin 3.1 software. All the NMR spectra were calibrated to the residual solvent signals.

Selected Equations

In the case of trivalent europium, the value of the radiative lifetime (τ_R) can be calculated using Eqn 1,

$$\frac{1}{\tau_R} = 14.65\ s^{-1} \times n^3 \times \frac{I_{Tot}}{I_{MI}} \quad (1)$$

where the value 14.65 s^{-1} is the spontaneous emission probability of the $^7F_1 \leftarrow {}^5D_0$ transition,[24] I_{Tot} is the total integration of the Eu^{3+} emission spectrum, I_{MD} is the integration of the $^7F_1 \leftarrow {}^5D_0$ transition and *n* is the refractive index of the solvent used or assumed value of 1.5 for the solid state.[25,26]

The intrinsic quantum yield (Φ_{Ln}^{Ln}) can be calculated using Eqn. 2,[24] where τ_{obs} is the observed excited state lifetime decay.

$$\Phi_{Ln}^{Ln} = \frac{\tau_{obs}}{\tau_R} \quad (2)$$

The sensitisation efficiency (η_{sens}) can be determined using Eqn.3:

$$\eta_{sens} = \frac{\Phi_{Ln}^{L}}{\Phi_{Ln}^{Ln}} \quad (3)$$

Overall quantum yields (Φ_{Ln}^{L}) in solution can be calculated using the optically dilute method proposed by Crosby and Demas[27], following Eqn 4:

$$\Phi_{Ln}^{L} = \Phi_{ref}\left(\frac{I_{Ln}}{I_{ref}}\right)\left(\frac{A_{ref}}{A_{Ln}}\right)\left(\frac{n_{Ln}^2}{n_{ref}^2}\right) \quad (4)$$

where Φ_{ref} is the photoluminescence quantum yield of the reference, *I* is the integrated area under the emission spectrum, *A* is the absorbance and *n* the refractive index.

Photophysical Measurements

Absorption spectra were recorded at room temperature using a Perkin Elmer Lambda 35 UV/Vis spectrometer. Uncorrected steady-state emission and excitation spectra were recorded using an Edinburgh FLSP980-stm spectrometer equipped with a 450 W xenon arc lamp, double excitation and emission monochromators, a Peltier-cooled Hamamatsu R928P photomultiplier (185–850 nm) and a Hamamatsu R5509-42 photomultiplier for detection of NIR radiation (800-1400 nm). Emission and excitation spectra were corrected for source intensity (lamp and grating) and emission spectral response (detector and grating) by a calibration curve supplied with the instrument.

Overall quantum yields in the solid-state were measured with the use of an integrating sphere coated with BenFlect. For the overall quantum yield of Yb^{3+} complexes the use of two different detectors, visible and NIR, is required. Therefore, a correction factor, as the ratio of the measured quantum yield to the reported value for a known sample, needs to be applied. To do that, [Yb(**phen**)(**tta**)$_3$], where tta is thenoyltrifluoroacetonate, with an overall quantum yield of 1.6% in toluene was used as the reference.[28]

Overall quantum yields in solution were determined by the optically dilute method[27] using Equation 4. Absorption and emission spectra were measured in 10^{-5} M dichloromethane solutions by excitation at 350 nm under the same experimental conditions as the standard; air-equilibrated water solution of [Ru(**bpy**)$_3$]Cl$_2$, where bpy is 2,2'-bipyridine, (Φ_{ref} =2.8%)[29] for Eu^{3+} and [Yb(**phen**)(**tta**)$_3$] in toluene (Φ^{L}_{Ln}=1.6%)[28] for the Yb^{3+} complexes. Experimental uncertainties are estimated to be ±10% for quantum yields.

Excited-state decays (τ) were recorded on the same Edinburgh FLSP980-stm spectrometer using a microsecond flashlamp. The goodness of fit was assessed by minimising the reduced χ^2 function and by visual inspection of the weighted residuals. Experimental uncertainties are estimated to be ±10%.

To record the luminescence spectra at 77 K, the samples were placed in quartz tubes (2 mm diameter) and inserted in a special quartz Dewar filled with liquid nitrogen. All the solvents used in the preparation of the solutions for the photophysical investigations were of spectrometric grade.

Synthesis

The [Ln(**phen**)(**tbm**)$_3$] (Ln^{3+} = Eu, Er, Yb) were prepared in a similar manner by reaction of **tbm**H (50 mg, 0.15 mmol), phen (9 mg, 0.05 mmol) and hydrated $LnCl_3$ (0.05 mmol) in ethanol (10 mL). Triethylamine (23 µL, 0.15 mmol) was added and the mixture was heated at 50 °C for 30 minutes. The resulting mixture was hot filtered and the filtrate left to stand at ambient temperature. Slow evaporation of the solvent over several days afforded yellow crystals in every case.

[Eu(**phen**)(**tbm**)$_3$]: 20 mg (0.015 mmol) 30%. M.p. 232-233 °C; elemental analysis calcd (%) for $C_{78}H_{53}N_2O_9Eu{\cdot}H_2O$: C, 70.32; H, 4.16 N, 2.10; found: C, 70.54; H, 4.09; N, 2.12 ATR-IR: *v* = 3058 w, 3024 w, 1642 m, 1583 s, 1537 s, 1448 m, 1428 m, 1366 s, 1310 m, 1292 m, 1275 m, 1176 w, 1154 m, 1101 w, 1072 w, 1027 w, 1013 w, 1000 w, 968 w, 920 w, 895 m, 863 w, 844 w, 823 w, 810 w, 780 w, 743 m, 729 w, 721 w, 692 m, 667 cm^{-1} w.

[Er(**phen**)(**tbm**)$_3$]: 18 mg (0.014 mmol), 28%. M.p. 248-249 °C; elemental analysis calcd (%) for $C_{78}H_{53}N_2O_9Er{\cdot}H_2O$: C, 69.52; H, 4.11; N, 2.08; found: C, 69.94; H, 3.65; N, 2.17; ATR-IR: *v* = 3058 w, 1642 m, 1565m, 1583 m, 1538 s, 1448 m, 1427 w, 1368 s, 1310 m, 1276 m, 1222 w, 1176 w, 1154 m, 1102 w, 1072 w, 1027 w, 1013 w, 1000 w, 968 w, 920 w, 896 m, 863 w, 843 w, 824 w, 810 w, 779 w, 742 m, 728 w, 722 w, 692 s, 666 cm^{-1} w.

[Yb(**phen**)(**tbm**)$_3$]: 30 mg (0.020 mmol), 45%. M.p. 256-257 °C; elemental analysis calcd (%) for $C_{78}H_{53}N_2O_9Yb{\cdot}H_2O$: C, 69.23; H, 4.10; N, 2.07: found: C, 69.28; H, 3.75; N, 2.01; ATR-IR: *v* = 3060 w, 1669 w, 1643 m, 1583 m, 1538 s, 1448 m, 1427 w, 1369 s, 1310 w, 1277 m, 1177 w, 1155 m, 1102 w, 1073 w, 1027 w, 1013 w, 1000 w, 968 w, 921 w, 896 m, 864 w, 844 w, 824 w, 811 w, 780 w, 759 m, 729 m, 723 m, 692 s, 667 cm^{-1} w.

PMMA materials

The lanthanoid complexes were dispersed into PMMA samples as described previously.[30]

Crystallography

Crystallographic data for the structures were collected at 100(2) K on an Oxford Diffraction Gemini or Xcalibur diffractometer fitted using Mo Kα or Cu Kα radiation**.** Following absorption corrections and solution by direct methods, the structures were refined against F^2 with full-matrix least-squares using the program SHELXL-97 or SHELX-2014.[31] Unless stated below, anisotropic displacement parameters were employed for the non-hydrogen atoms and hydrogen atoms were added at calculated positions and refined by use of a riding model with isotropic displacement parameters based on those of the parent atom. CCDC-1401032 [Eu(**phen**)(**tbm**)$_3$], CCDC- 3000194 [Er(**phen**)(**tbm**)$_3$], CCDC- 1587889 [Yb(**phen**)(**tbm**)$_3$] and CCDC- 3000195 [Ho(**tbm**)$_3$(EtOH)(H$_2$O).1/2(EtOH] contain supplementary crystallographic data, and can be obtained free of charge *via* http://www.ccdc.cam.ac.uk/conts/retrieving.html, or from the Cambridge Crystallographic Data Centre, 12 Union Road, Cambridge CB2 1EZ, U.K.; fax: (+44) 1223-336-033; or e-mail: deposit@ccdc.cam.ac.uk

[Eu(**phen**)(**tbm**)$_3$]

Empirical formula $C_{78}H_{53}EuN_2O_9$; *MW* = 1314.18. λ = 0.71073 Å. Triclinic, Space group *P*1,¯, *a* = 10.5972(3), *b* = 13.5765(3), *c* = 21.3722(5) Å, α = 93.095(2)°, β = 102.252(2)°, γ = 95.526(2)°, Volume = 2982.11(13) $Å^3$, *Z* = 2; ρ_c = 1.464 Mg/m^3, µ = 1.117 mm^{-1}, crystal size 0.35 x 0.12 x 0.12 mm3; $\theta_{min,\ max}$ = 2.35, 32.73°. Reflections collected = 64852, unique reflections = 20096 [*R*(int) = 0.0355]. Max. and min. transmission = 0.892 and 0.768. Number of parameters = 811, S = 1.044. Final *R* indices [$I>2\sigma(I)$] *R*1 = 0.0287, *wR*2 = 0.0605; *R* indices (all data) *R*1 = 0.0356, *wR*2 = 0.0633. Largest diff. peak and hole = 0.874 and -0.516 e. $Å^{-3}$.

[Er(**phen**)(**tbm**)$_3$]

Empirical formula $C_{78}H_{53}ErN_2O_9$; *MW* = 1329.48. λ = 1.54178. Triclinic, Space group *P*1,¯, *a* = 10.6127(3), *b* = 13.4533(4), *c* = 21.3672(7) Å, α = 93.073(2)°, β = 102.241(2)°, γ = 96.098(2)°, Volume = 2955.38(16) $Å^3$, *Z* = 2; ρ_c = 1.493 Mg/m^3, µ = 3.169 mm^{-1}, crystal size 0.15 x 0.07 x 0.05 mm^3; $\theta_{min,\ max}$ = 3.31, 67.27°. Reflections collected = 26571, unique reflections =

10450 [*R*(int) = 0.0484]. Max. and min. transmission = 0.864 and 0.738. Number of parameters = 811, S = 1.000. Final *R* indices [*I*>2σ(*I*)] *R*1 = 0.0460, *wR*2 = 0.1261; *R* indices (all data) *R*1 = 0.0561, *wR*2 = 0.1332. Largest diff. peak and hole = 1.45 and -0.80 e. Å^{-3}.

[Yb(**phen**)(**tbm**)$_3$]
Empirical formula $C_{78}H_{53}YbN_2O_9$; MW = 1335.26. λ = 0.71073 Å. Triclinic, Space group P1,$^{-}$, *a* = 10.6346(4), *b* = 13.4190(4), *c* = 21.3553(7) Å, α = 93.181(2)°, β = 102.149(3)°, γ = 96.363(3)°, Volume = 2951.16(18) Å^3, *Z* = 2; ρ_c = 1.503 Mg/m^3, μ = 1.651 mm^{-1}, crystal size 0.39 x 0.19 x 0.105 mm^3; $\theta_{min,\ max}$ = 2.342, 30.00°. Reflections collected = 31453, unique reflections = 17169 [*R*(int) = 0.0370]. Max. and min. transmission = 0.852 and 0.649. Number of parameters = 812, S = 1.037. Final *R* indices [*I*>2σ(*I*)] *R*1 = 0.0389, *wR*2 = 0.0758; *R* indices (all data) *R*1 = 0.0487, *wR*2 = 0.0799. Largest diff. peak and hole = 1.805 and -0.803 e. Å^{-3}.

[Ho(**tbm**)$_3$(EtOH)(H$_2$O)]
Empirical formula $C_{69}H_{56}HoO_{11.50}$; *MW* = 1234.07. λ = 0.71073 Å. Triclinic, Space group *P*1,$^{-}$, *a* = 12.7743(4), *b* = 13.8632(4), *c* = 17.0964(4) Å, α = 100.360(2)°, β = 100.374(2)°, γ = 102.132(3)°, Volume = 2836.07(14) Å^3, *Z* = 2; ρ_c = 1.445 Mg/m^3, μ = 1.460 mm^{-1}, crystal size 0.40 x 0.18 x 0.15 mm^3; $\theta_{min,\ max}$ = 3.01, 33.00°. Reflections collected = 78818, unique reflections = 21339 [*R*(int) = 0.0354]. Max. and min. transmission = 0.832 and 0.674. Number of parameters = 763, S = 1.088; Final R indices [*I*>2σ(*I*)] *R*1 = 0.0503, *wR*2 = 0.1237; R indices (all data) *R*1 = 0.0603, *wR*2 = 0.1294; Largest diff. peak and hole 4.897 and -2.881 e. Å^{-3}. The methyl group of the coordinated ethanol molecule was modelled as being disordered over two sites with occupancies constrained to 0.5 after trial refinement. The site occupancy of the solvent ethanol molecule was constrained to 0.5 from trial refinement and molecular interaction considerations. The water molecule and ethanol hydrogen atoms were located and refined with geometries restrained to ideal values.

Results and discussion

Tribenzoylmethane (**tbm**H) was synthesised according to a literature procedure,[20] whereby dibenzoylmethane (**dbm**H) was reacted with benzoyl chloride and NaH in dry diethyl ether.

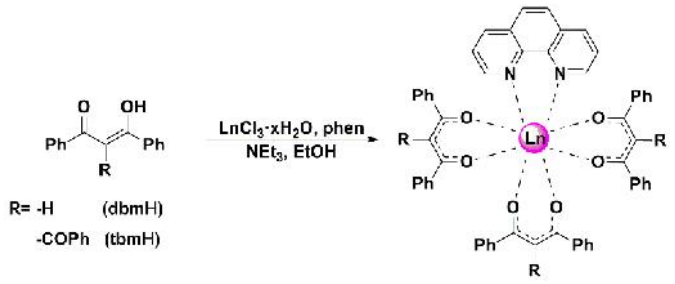

Figure 1 - Reaction scheme for the preparation of [Ln(**phen**)(**dbm**)$_3$] and [Ln(**phen**)(**tbm**)$_3$] (Ln= Eu^{3+}, Er^{3+}, Yb^{3+} complexes).

Previous methods for the synthesis of β-triketonate complexes present two alternatives: the use of alkali hydroxides to form the tetranuclear assemblies,[20–22] or triethylamine, which results in mononuclear complexes.[32] However, in the latter work reported by Ismail *et al.*, the complex formulated as [Eu(**tbm**)$_3$(HOEt)(H$_2$O)] was assigned only from elemental and thermal analyses in the absence of any structural characterisation *via* X-ray diffraction.[32] In an attempt to synthesise and crystallise analogous mononuclear complexes with the use of triethylamine, hydrated $LnCl_3$ salts (Ln = La^{3+}, Tb^{3+}, Dy^{3+}, Ho^{3+}, Yb^{3+}) were reacted with three equivalents of **tbm**H and triethylamine in ethanol at 50 °C. An appropriately crystalline product was only obtained in the case of $HoCl_3$, where slow evaporation of the solvent over several days resulted in the formation of yellow single crystals. Analysis of the product by single crystal X-ray diffraction revealed the first structurally characterised mononuclear triketonate structure, [Ho(**tbm**)$_3$(HOEt)(H$_2$O)]·EtOH, consistent with the composition proposed by Ismail *et al.*[32] (see Electronic Supporting Information). In the other cases, only amorphous powders were obtained with analogous spectroscopic data.

While this result confirmed the structures first assigned to these complexes, it was necessary to remove solvent molecules from the first coordination sphere to improve their photophysical properties. Hence, [Ln(**phen**)(**dbm**)$_3$] and [Ln(**phen**)(**tbm**)$_3$] complexes (Ln = Eu^{3+}, Er^{3+}, Yb^{3+}) were prepared by the addition of **tbm**H, **phen**, and hydrated $LnCl_3$ with triethylamine to hot ethanol (Figure 1). After filtration, slow evaporation of the solvent resulted in the formation of suitable crystals for X-ray diffraction for the [Ln(**phen**)(**tbm**)$_3$] (Ln^{3+} = Eu^{3+}, Er^{3+}, Yb^{3+}). The formulation of the resulting solids was confirmed by elemental analysis and IR spectroscopy.

The previously reported [Ln(**phen**)(**dbm**)$_3$] complexes were prepared following a slightly modified procedure.[33] Reaction of **dbm**H, **phen**, and hydrated $LnCl_3$ with triethylamine in ethanol at 50 °C resulted in pale yellow solids, which were filtered, washed with ethanol and dried *in vacuo*. The formulation of the resulting solids was supported by elemental analysis, with the consistent inclusion of one equivalent of water, presumably incorporated from atmospheric water upon isolation of the crystals from solution.

X-ray diffraction studies

The [Ln(**phen**)(**tbm**)$_3$] (Ln = Eu^{3+}, Er^{3+}, Yb^{3+}) complexes are isostructural, crystallising as triclinic structures in the *P*1,$^{-}$ space group (Figure 2). The Ln^{3+} cations are eight-coordinate by six O atoms from three **tbm** ligands and two N atoms from the coordinated **phen** molecule. The coordination geometry is best described as a distorted square antiprism. A supramolecular dimer, situated about an inversion centre, is formed through π-stacking[34] of **phen** ligands of two adjacent complexes, with a distance of ~3.26 Å between the π-stacked planes of the **phen** ligands. These interactions result in a Ln···Ln distance in a range of 9.21-9.25 Å, a distance which

suggests that direct energy transfer between the two Ln^{3+} ions should be minimal.[35]

Table 1 - Selected bond lengths (Å) and intermetallic distances for [Ln(phen)**(tbm)**$_3$].

	[Eu(phen)(tbm)$_3$]	[Er(phen)(tbm)$_3$]	[Yb(phen)(tbm)$_3$]
Ln(1)-N(421)	2.583(1)	2.510(4)	2.495(2)
Ln(1)-N(411)	2.602(1)	2.545(4)	2.523(2)
Ln(1)-O(11)	2.330(1)	2.260(3)	2.252(2)
Ln(1)-O(12)	2.372(1)	2.306(3)	2.287(2)
Ln(1)-O(21)	2.333(1)	2.282(3)	2.254(2)
Ln(1)-O(22)	2.367(1)	2.305(3)	2.295(2)
Ln(1)-O(31)	2.394(1)	2.342(3)	2.322(2)
Ln(1)-O(32)	2.338(1)	2.287(3)	2.261(2)
phen-phen	3.292(3)	3.263(7)	3.256(4)
Centroid-Centroid	3.605	3.411	3.410
Ln(1)-Ln(2)	9.2508(6)	9.2357(6)	9.2141(6)

The [Ln(**phen**)(**dbm**)$_3$] (Ln = Eu^{3+}, Er^{3+}, Yb^{3+}) crystal structures have been previously reported in the literature.[33,36,37] Similarly to the [Ln(**phen**)(**tbm**)$_3$] complexes, the Ln^{3+} ion is coordinated by six O atoms from three **dbm** ligands and two N atoms from the coordinated **phen** molecule. Unlike the **tbm** series, the **dbm** complexes are not isomorphous. Nevertheless, the Ln···Ln distances are greater than 9 Å in all of these complexes and thus cross relaxation pathways are not expected to influence one series of complexes more than the other in the solid state.

Most importantly for this study, the coordination spheres of the complexes of each lanthanoid cation are quite similar. Overlaying the primary coordination sphere structures[38] for the **dbm** and **tbm** complexes of each metal gave RMSD for the overlay and the maximum distance between two equivalent atoms (Max. D) as follows: Eu, RMSD 0.1230, Max D 0.1964; Er, RSMD 0.0939, Max D 0.1338; Yb, RMSD 0.2146, Max D 0.3583 Å. The overlaid structures are shown in the Supporting Information. Shape analysis,[39] comparing the distortion from idealised coordination geometries, were consistent with these results, with the Yb pair of complexes showing the greatest differences in structure.

Photophysical investigation

The photophysical properties for [Ln(**phen**)(**tbm**)$_3$] (Ln = Eu^{3+} and Yb^{3+}) including excited state lifetime decays (τ_{obs}), calculated radiative lifetime decays (τ_R), intrinsic photoluminescence quantum yields (Φ_{Ln}^{Ln}), overall photoluminescence quantum yields (Φ_{Ln}^{L}), and sensitisation efficiency (η_{sens}) are summarised in Table 2.

The energies of the $^3\pi\pi^*$ excited states of the **dbm**[40] and **tbm** ligands were estimated at the 0-phonon transition from the phosphorescence of the Gd^{3+} complexes in a frozen dichloromethane solution at 77 K. These energies were calculated to be 20,350 cm^{-1} and 20,704 cm^{-1}, respectively, in agreement with the literature values.[20,41] The $^3\pi\pi^*$ state energy of the **phen** ligand has been previously reported at 21,050 cm^{-1} in the presence of hydrated $GdCl_3$.[42,43] These $^3\pi\pi^*$

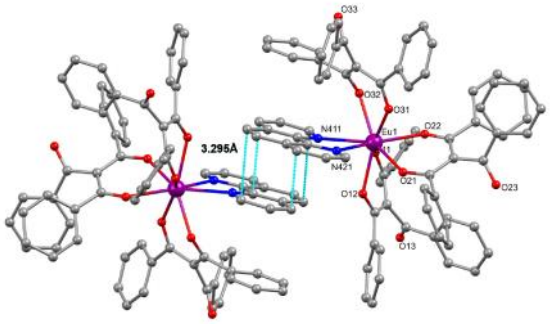

Figure 2 - A ball and stick representation of the X-ray crystal structure of [Eu(**phen**)(**tbm**)$_3$], emphasising the supramolecular dimer formed by phen π-π stacking interactions between centrosymmetrically related molecules. Hydrogen atoms have been omitted for clarity.

states are of high enough energy to sensitise NIR metal-centred emission from Er^{3+} and Yb^{3+}. The similarities between the excitation spectra and the absorption profiles of the **tbm**/**dbm** ligands and **phen** ligands support the conclusion that the emission from the lanthanoid cations originates through sensitisation from the coordinated ligands (see Supporting Information). Given the large energy difference between the energy of the $^3\pi\pi^*$ and $^2F_{5/2}$ excited state of Yb^{3+}, energy transfer in this case could be mediated by a ligand-to-metal charge transfer state (LMCT).[44] In the case of Eu^{3+}, energy transfer will usually occur to the $^5D_0$ (~17,200 cm^{-1}) or $^5D_1$ (~19,000 cm^{-1}) states.[45] Sato and Wada have reported that for efficient funnelling of the energy to the $^5D_1$ state, an energy difference of 1,500 cm^{-1} is sufficient.[7] Therefore in our systems, energy transfer is likely to occur to both excited states.

The measurements were performed on neat solids or with the complexes dispersed within a transparent PMMA matrix following a previously reported procedure.[30] The obtained data were also compared with measurements performed in *ca.* 10^{-5} M dichloromethane solutions at room temperature and at 77 K. Dichloromethane was used as a non-coordinating solvent, as the structure was not preserved in polar coordinating solvents such as ethanol due to ligand exchange (see Supporting Information). The photophysical properties of [Er(**phen**)(**tbm**)$_3$] were only studied in the solid state as this complex was almost non-emissive from solution at room temperature (see Supporting Information).

Europium Complexes. The combined emission spectra for the Eu^{3+} complexes are shown in Figure 3. The emission spectrum of [Eu(**phen**)(**tbm**)$_3$] in the solid state displays the five characteristic Eu^{3+} emission bands attributed to $^7F_J \leftarrow {}^5D_0$ (J = 0-4) transitions in the region of 580-750 nm. The low intensity $^7F_0 \leftarrow {}^5D_0$ band has a full-width at half-maximum (FWHM) of 35

Table 2. Photophysical data for [Ln(**phen**)(**tbm**)$_3$] and [Ln(**phen**)(**dbm**)$_3$] complexes.

Complex	Environment	τ_{obs} (μs)	τ_R (μs)	Φ_{Ln}^{Ln} (%)	Φ_{Ln}^{L} (%)	η_{sens}(%)
[Eu(phen)(**tbm**)$_3$]	Solid State	550	1030	53	45[a]	85
	DCM (RT)	124	1080	12	0.6[b]	5
	DCM glass (77K)	554	990	56	-	-
	PMMA	433	1009	43	-	-
[Eu(phen)(**dbm**)$_3$]	Solid State	484	960	50	55[a]	~100
	DCM (RT)	120	843	14	1.3[b]	10
	DCM glass (77K)	673	989	68	-	-
	PMMA	462	956	48	-	-
[Yb(phen)(**tbm**)$_3$]	Solid State	15.9	-	-	3.64[a]	-
	DCM RT)	18.0	-	-	1.16[c]	-
	DCM glass (77K)	16.0	-	-	-	-
	PMMA	16.7	-	-	-	-
[Yb(phen)(**dbm**)$_3$]	Solid State	11.3	-	-	2.91[a]	-
	DCM (RT)	12.9	-	-	0.87[c]	-
	DCM glass (77K)	9.7	-	-	-	-
	PMMA	10.7	-	-	-	-

[a] quantum yield measured with an integrating sphere; [b] quantum yield in dichloromethane solution relative to [Ru(**bpy**)$_3$]Cl$_2$ in water (Φ_{ref} =2.8%)[29]; [c] quantum yield in dichloromethane solution relative to [Yb(**phen**)(**TTA**)$_3$] in toluene (Φ^{L}_{Ln}=1.6%)[28]. See Experimental Section for details on the standard used.

cm^{-1}, indicative of one unique emitting species.[46] The $^7F_1 \leftarrow {}^5D_0$ transition is split into three easily distinguishable bands, two of which are very close in energy. This splitting is inherent for a local Eu^{3+} symmetry lower than D_{2d}.[46] This is consistent with the observed splitting in the $^7F_2 \leftarrow {}^5D_0$ band and the high integral ratio (13.5) of this band with respect to the $^7F_1 \leftarrow {}^5D_0$. Low symmetry is observed as well in the crystal structure where the ideal square antiprismatic geometry is distorted, with a symmetry lowered due to the *N*-donor ligand.

The emission spectrum for the [Eu(**phen**)(**dbm**)$_3$] in the solid state is in agreement with the literature, showing the five characteristic Eu^{3+} bands associated with $^7F_J \leftarrow {}^5D_0$ (J = 0-4) transitions. The $^7F_0 \leftarrow {}^5D_0$ band has a FWHM of 27 cm^{-1}, which again indicates the presence of only one unique emitting Eu^{3+} centre. The $^7F_1 \leftarrow {}^5D_0$ transition is split in two different bands because of the crystal field effects. The splitting of the band is lower than for [Eu(**phen**)(**tbm**)$_3$], revealing higher symmetry in this case, which is in agreement with the results found with the shape analysis, where the [Eu(**phen**)(**dbm**)$_3$] complex is less distorted from square antiprismatic geometry compared to the analogous complexes bound to **tbm** (see Supporting Information).[39]

The [Eu(**phen**)(**tbm**)$_3$] excited state decay was found to be monoexponentional (see Supporting Information), giving an excited state lifetime (τ_{obs}) value of 0.55 ms. The radiative decay (τ_R) could be estimated from the emission spectrum to be 1.03 ms. From these data, the intrinsic quantum yield (Φ_{Ln}^{Ln}) was calculated to be 53%. The overall quantum yield was measured to be 45% by an absolute method using an integrating sphere, leading to a sensitisation efficiency (η_{sens}) of 82%. This value is slightly improved in comparison to our previous report on the assemblies that involved only **tbm** ligands (~70%),[21] and thus may be due to more efficient sensitisation *via* the **phen** ligand upon excitation at 350 nm. The values of τ_{obs}, τ_R, and Φ_{Ln}^{Ln} for the [Eu(**phen**)(**dbm**)$_3$] were found to be very similar to the **tbm** complex at 0.48 ms, 0.96 ms and 50%, respectively, with an overall quantum yield (Φ_{Ln}^{L}) of 55% and a virtually quantitative sensitisation efficiency, within experimental error, associated with the quantum yield measurement. These data indicate that the introduction of the extra ketone group at the α-carbon of the β-diketone does not significantly affect the emission behaviour for Eu^{3+} complexes, and the photophysical properties for the β-diketonate and β-triketonate complexes are comparable. This is not surprising, as the α-CH bond is not an efficient quencher of the $^5D_0$ excited state.

As both systems behave similarly across every medium, and the data for the [Eu(**phen**)(**dbm**)$_3$] are in agreement with the literature,[33] only the photophysical properties of the [Eu(**phen**)(**tbm**)$_3$] complexes will be discussed from here on.

The emission properties of [Eu(**phen**)(**tbm**)$_3$] and [Eu(**phen**)(**dbm**)$_3$] in PMMA were studied in order to assess any possible contribution of energy migration between Eu^{3+} centres in the neat solid. Only in the case of [Eu(**phen**)(**tbm**)$_3$] was there an indication of slightly different splitting of emission bands compared to the solid state that may be due to a different geometry of the ligands around the lanthanoid centre in the dispersed medium. The values of τ_{obs}, τ_R, and Φ_{Ln}^{Ln}

are 0.43 ms, 1.09 ms, and 43%, respectively. These data show similar values to those in neat solids, suggesting that concentration quenching does not affect the solid-state emission properties.

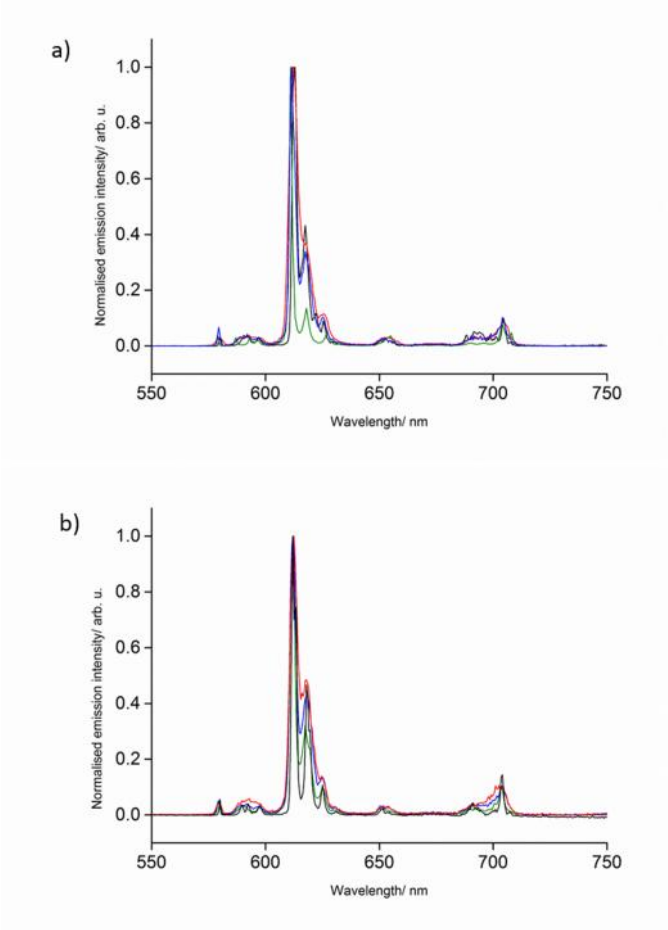

Figure 3 - Normalised emission plots for a) [Eu(**phen**)(**tbm**)$_3$] and b) [Eu(**phen**)(**dbm**)$_3$] in solid state (green trace), DCM solution(10-5M) (red trace), 77K (black trace) and PMMA (blue trace), with excitation wavelength at 350 nm.

The [Eu(**phen**)(**tbm**)$_3$] complex in dichloromethane solution at room temperature shows characteristic emission from the Eu^{3+} $^5D_0$ state, similar to the spectrum observed in PMMA. All the emission lines were less defined due to higher degrees of freedom of the ligands in solution at room temperature. However, when the solution formed a glass at 77 K, the emission structure was similar to that observed in PMMA with no significant changes. The FWHM of the $^7F_0 \leftarrow ^5D_0$ transition are 82 cm^{-1} and 26 cm^{-1} at room temperature and 77 K, respectively. In the frozen glass, the $^7F_1 \leftarrow ^5D_0$ transition is split into three bands, two of them very close in energy comparable to the dispersed medium.

Excited state lifetime decays (τ_{obs}) of [Eu(**phen**)(**tbm**)$_3$] in dichloromethane solution were measured to be 0.12 ms and 0.55 ms at room temperature and 77 K, respectively (see Supporting Information). The radiative decay (τ_R), the intrinsic (Φ_{Ln}^{Ln}) and overall quantum yield (Φ_{Ln}^{L}) at room temperature were determined to be 1.08 ms, 12% and 0.58%, which leads to a sensitisation efficiency (η_{sens}) of 5%. These data are consistent with those reported for [Eu(**phen**)(**dbm**)$_3$] in dichloromethane solution, suggesting similar behaviour of both systems in solution. The significantly short lifetimes found at room temperature with respect to the 77K may be explained by a more efficient vibrational quenching of the $^5D_0$ excited state favoured due to a higher configurational lability in solution. The reduction in the overall quantum yield, in comparison to that in the solid state, is suggestive of a poor sensitisation efficiency of the ketonates in solution which may suggest quenching of the triplet state of **tbm** in agreement with previous literature.[33]

These results demonstrate that both β-diketonate and β-triketonate systems behave similarly in every media, thereby confirming that the α-CH bond is not an efficient quencher of the $^5D_0$ excited state. However, the poor emission properties of both systems in solution, in comparison with the neat solids, suggest efficient quenching processes taking place and poor sensitisation properties of these ketonates.

Ytterbium complexes. The combined emission spectra for the Yb^{3+} complexes are shown in Figure 4. The emission spectrum of the [Yb(**phen**)(**tbm**)$_3$] complex in the solid state shows characteristic NIR emission from the $^2F_{7/2} \leftarrow ^2F_{5/2}$. This transition is split into four main bands at 976, 1011, 1029 and 1043 nm due to crystal field effects. The splitting of the $^2F_{7/2} \leftarrow ^2F_{5/2}$ transition in the case of the [Yb(**phen**)(**dbm**)$_3$] is slightly different with three main bands at 976, 1007 and 1039 nm. This may be due to different degrees of distortion between the two coordination spheres, which were the largest differences observed amongst the three pairs of complexes. This is also in accordance with the results found in the shape analysis study, where it was shown that [Yb(**phen**)(**tbm**)$_3$] is best described as a distorted square antiprism, while the best description of the geometry for [Yb(**phen**)(**dbm**)$_3$] is a distorted triangular dodecahedron (see Supporting Information).

The observed lifetime decays (τ_{obs}) for [Yb(**phen**)(**tbm**)$_3$] and [Yb(**phen**)(**dbm**)$_3$] complexes in the solid state were fitted to monoexponential functions, giving values of 15.9 and 11.3 μs, respectively. The excited state lifetime is slightly higher in the case of the [Yb(**phen**)(**tbm**)$_3$]. Overall quantum yields (Φ_{Ln}^{L}) were measured with the help of an integrating sphere using two different detectors: visible and NIR. In order to do so, [Yb(**phen**)(**tta**)$_3$] with Φ_{Ln}^{L}=1.6%,[28] was used as a reference to calibrate the system. The value of Φ_{Ln}^{L} for the previous reported complex, [Yb(**phen**)(**dbm**)$_3$] in toluene was found to be 0.62%, in accordance with the literature value of 0.59%.[28] The Φ_{Ln}^{L} of the [Yb(**phen**)(**tbm**)$_3$] and [Yb(**phen**)(**dbm**)$_3$] in the solid state were determined to be 3.64 and 2.91%, respectively, showing a small enhancement for the **tbm** complex due to reduction of non-radiative decay pathways.[20]

As for the Eu^{3+} complexes, the photophysical properties of the [Yb(**phen**)(**tbm**)$_3$] and [Yb(**phen**)(**dbm**)$_3$] in PMMA were

studied. The emission spectrum of [Yb(**phen**)(**tbm**)$_3$] shows emission from the $^2F_{7/2}\leftarrow{}^2F_{5/2}$ transition with a slightly different splitting of the band due to small differences in the coordination sphere. The values of observed lifetimes decay (τ_{obs}) are similar to the ones found in the solid state.

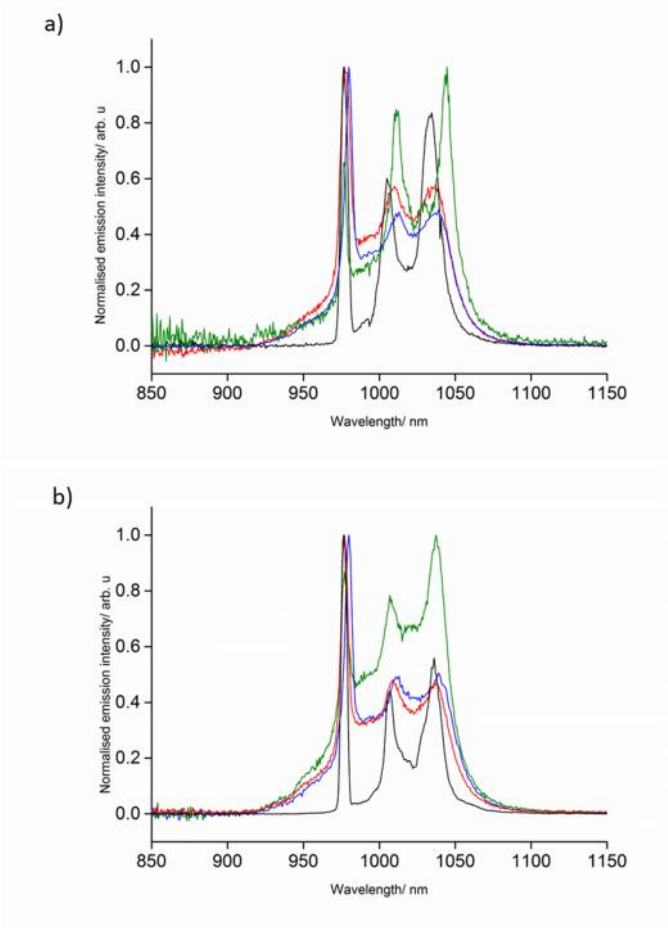

Figure 4.- Normalised emission plots for a) [Yb(**phen**)(**tbm**)$_3$] and b) [Yb(**phen**)(**dbm**)$_3$] in solid state (green trace), DCM solution(10-5M) (red trace), 77K (back trace) and PMMA (blue trace), with excitation wavelength at 350nm.

The [Yb(**phen**)(**tbm**)$_3$] and [Yb(**phen**)(**dbm**)$_3$] complexes in dichloromethane solution at room temperature and at 77 K show characteristic emission from the $^2F_{5/2}$ state with a similar splitting to the spectra observed in PMMA. The observed lifetime decays (τ_{obs}) were fitted to monoexponential functions with values of 18.0 and 12.9 µs, respectively (see Supporting Information). The overall quantum yield (Φ_{Ln}^{L}) of the [Yb(**phen**)(**tbm**)$_3$] and [Yb(**phen**)(**dbm**)$_3$] at room temperature were determined to be 1.16 and 0.87%, respectively, by the dilute method using [Yb(phen)(tta)$_3$] as the reference.[28] The values of the quantum yields are slightly lower than in the solid state probably due to a less efficient sensitisation process, as was seen to a greater degree for the Eu^{3+} complexes. These data suggest that energy migration between the lanthanoid centres does not affect the photophysical properties of the complexes in the neat solids.

These results indicate that the additional ketone group at the α-carbon of the β-diketone has an effect on the emission behaviour for Yb^{3+} complexes, and the photophysical properties for the β-triketonate complexes are slightly enhanced. That is not surprising because the α-CH bond is an efficient quencher of the $^2F_{5/2}$ excited state. However, the values found for the monomeric species do not rival the photophysics of the previously reported tetranuclear assemblies, suggesting that the assemblies present an environment strongly protected from multiphonon relaxation.

Conclusions

We report here, three new mononuclear eight-coordinate Eu^{3+}, Er^{3+} and Yb^{3+} complexes with tribenzoylmethanide (**tbm**) and phenanthroline (**phen**) ligands, of the general formula [Ln(**phen**)(**tbm**)$_3$]. This work has focussed on a direct comparison with the analogous [Ln(**phen**)(**dbm**)$_3$] complexes, in order to better understand the effect on the photophysical properties of the replacement of the α-CH in β-diketonates with an additional ketone functional group to give β-triketonates.

The emission profiles, excited state lifetimes and quantum yields for Eu^{3+} revealed similar behaviour for both systems. Particularly short lifetimes were found in solution, suggestive of efficient deactivation pathways of the excited states via non-radiative decay. On the other hand, a small enhancement was observed for Yb^{3+} moving from the **dbm** to the **tbm** system, probably because of reduced multiphoton quenching. However, these values do not rival the photophysical properties of the previously reported assemblies[20–22], suggesting that simply replacing β-diketonates with β-triketonate ligands in similar complex structures is not likely to enhance photophysical properties. The remarkable properties of the tetranuclear assemblies presumably are linked to other factors that arise from their structure and composition.

Conflicts of interest

The authors declare no conflict of interest.

Acknowledgements

This research was partially supported by the Australian Research Council's Discovery *Projects* funding scheme (project DP17010189), and a Royal International Exchanges Grant. L.A.G and B.L.R. thanks Curtin University for the Australian Postgraduate Award and the University of Montreal (UdeM). G.S.H. thanks the Natural Sciences and Engineering Research Council of Canada and the Direction des Relations Internationales of UdeM. E.Z.-C. thanks the EPSRC (EP/M02105X/1) for support. The authors acknowledge access to the facilities at the Centre for Microscopy, Characterisation and Analysis, University of Western Australia.

Notes and references

1 S. V. Eliseeva and J.-C. G. Bünzli, *Chem. Soc. Rev.*, 2010, **39**, 189–227.

2 S. V. Eliseeva and J.-C. G. Bünzli, *New J. Chem.*, 2011, **35**, 1165.

3 J.-C. G. Bünzli and S. V. Eliseeva, *J. Rare Earths*, 2010, **28**, 824–842.

4 J. Andres, R. D. Hersch, J.-E. Moser and A.-S. Chauvin, *Adv. Funct. Mater.*, 2014, **24**, 5029–5036.

5 S. Faulkner, S. J. A. Pope and B. P. Burton-Pye, *Appl. Spectrosc. Rev.*, 2005, **40**, 1–31.

6 F. J. Steemers, W. Verboom, D. N. Reinhoudt, E. B. Vandertol and J. W. Verhoeven, *J. Am. Chem. Soc.*, 1995, **117**, 9408–9414.

7 S. Sato and M. Wada, *Bull. Chem. Soc. Jpn.*, 1970, **43**, 1955–1962.

8 J. G. Bunzli and S. V Eliseeva, *Springer Ser. Fluoresc.*, 2011, 1–45.

9 A. Beeby, R. S. Dickins, S. Faulkner, D. Parker and J. A. Gareth Williams, *Chem. Commun.*, 1997, 1401–1402.

10 S. Faulkner, A. Beeby, M.-C. Carrié, A. Dadabhoy, A. M. Kenwright and P. G. Sammes, *Inorg. Chem. Commun.*, 2001, **4**, 187–190.

11 A. de Bettencourt-Dias, 2014, 378.

12 A. de Bettencourt-Dias, *Dalton Trans.*, 2007, 2229–2241.

13 K. Binnemans, 2005, **35**, 107–272.

14 Y. Hou, J. Shi, W. Chu and Z. Sun, *Eur. J. Inorg. Chem.*, 2013, **2013**, 3063–3069.

15 S. Biju, Y. K. Eom, J.-C. G. Bünzli and H. K. Kim, *J. Mater. Chem. C*, 2013, **1**, 6935.

16 M. L. P. Reddy, V. Divya and R. Pavithran, *Dalt. Trans.*, 2013, **42**, 15249.

17 A. P. Bassett, R. Van Deun, P. Nockemann, P. B. Glover, B. M. Kariuki, K. Van Hecke, L. Van Meervelt and Z. Pikramenou, *Inorg. Chem.*, 2005, **44**, 6140–6142.

18 P. B. Glover, A. P. Bassett, P. Nockemann, B. M. Kariuki, R. Van Deun and Z. Pikramenou, *Chem. - A Eur. J.*, 2007, **13**, 6308–6320.

19 K. Singh, R. Boddula and S. Vaidyanathan, *Inorg. Chem.*, 2017, **56**, 9376–9390.

20 B. L. Reid, S. Stagni, J. M. Malicka, M. Cocchi, G. S. Hanan, M. I. Ogden and M. Massi, *Chem. Commun.*, 2014, **50**, 11580–11582.

21 B. L. Reid, S. Stagni, J. M. Malicka, M. Cocchi, A. N. Sobolev, B. W. Skelton, E. G. Moore, G. S. Hanan, M. I. Ogden and M. Massi, *Chem. - A Eur. J.*, 2015, 1–11.

22 L. Abad Galan, B. L. Reid, S. Stagni, A. N. Sobolev, B. W. Skelton, M. Cocchi, J. M. Malicka, E. Zysman-colman, E. G. Moore, M. I. Ogden and M. Massi, *Inorg. Chem.*, 2017, **56**, 8975–8985.

23 V. S. Sastri, J.-C. G. Bünzli, V. R. Rao, G. V. S. Rayudu and J. R. Perumareddi, in *Modern Aspects of Rare Earths and Their Complexes*, Elsevier, 2003, pp. 259–374.

24 S. I. Klink, G. A. Hebbink, L. Grave, P. G. B. Oude Alink, F. C. J. M. van Veggel and M. H. V. Werts, *J. Phys. Chem. A*, 2002, **106**, 3681–3689.

25 N. M. Shavaleev, S. V Eliseeva, R. Scopelliti and J.-C. G. Bünzli, *Inorg. Chem.*, 2014, **53**, 5171–5178.

26 N. M. Shavaleev, S. V. Eliseeva, R. Scopelliti and J.-C. G. Bünzli, *Chem. - A Eur. J.*, 2009, **15**, 10790–10802.

27 G. a. Crosby and J. N. Demas, *J. Phys. Chem.*, 1971, **75**, 991–1024.

28 M. P. Tsvirko, S. B. Meshkova, V. Y. Venchikov, Z. M. Topilova and D. V. Bol'shoi, *Opt. Spectrosc.*, 2001, **90**, 669–673.

29 K. Nakamaru, *Bull. Chem. Soc. Jpn.*, 1982, 55, 2697–2705.

30 C. R. Driscoll, B. L. Reid, M. J. McIldowie, S. Muzzioli, G. L. Nealon, B. W. Skelton, S. Stagni, D. H. Brown, M. Massi and M. I. Ogden, *Chem. Commun. (Camb).*, 2011, **47**, 3876–3878.

31 G. M. Sheldrick, *Acta Crystallogr. Sect. C-Struct. Chem.*, 2015, **71**, 3–8.

32 M. Ismail, S. J. Lyle and J. E. Newbery, *J. Inorg. Nucl. Chem.*, 1969, **31**, 2091–2093.

33 J.-G. Bünzli, E. Moret, V. Foiret, K. J. Schenk, W. Mingzhao and Jin Linpei, *J. Alloys Compd.*, 1994, **207**–**208**, 107–111.

34 C. Janiak, *J. Chem. Soc. Dalton Trans.*, 2000, **0**, 3885–3896.

35 N. M. Shavaleev, R. Scopelliti, F. Gumy and J. C. G. Bünzli, *Inorg. Chem.*, 2009, **48**, 7937–7946.

36 L.-N. Sun, H.-J. Zhang, L.-S. Fu, F.-Y. Liu, Q.-G. Meng, C.-Y. Peng and J.-B. Yu, *Adv. Funct. Mater.*, 2005, **15**, 1041–1048.

37 L. N. Sun, H. J. Zhang, Q. G. Meng, F. Y. Liu, L. S. Fu, C. Y. Peng, J. B. Yu, G. L. Zheng and S. Bin Wang, *J. Phys. Chem. B*, 2005, **109**, 6174–6182.

38 C. F. Macrae, I. J. Bruno, J. A. Chisholm, P. R. Edgington, P. McCabe, E. Pidcock, L. Rodriguez-Monge, R. Taylor, J. Van De Streek and P. A. Wood, *J. Appl. Crystallogr.*, 2008, **41**, 466–470.

39 D. Casanova, M. Llunell, P. Alemany and S. Alvarez, *Chem. - A Eur. J.*, 2005, **11**, 1479–1494.

40 G. A. Crosby, R. E. Whan and R. M. Alire, *J. Chem. Phys.*, 1961, **34**, 743–748.

41 G. Zucchi, O. Maury, P. Thuéry and M. Ephritikhine, *Inorg. Chem.*, 2008, **47**, 10398–10406.

42 K. Zhuravlev, V. Tsaryuk, V. Kudryashova, I. Pekareva, J. Sokolnicki and Y. Yakovlev, *J. Lumin.*, 2010, **130**, 1489–1496.

43 N. Armaroli, L. De Cola, V. Balzani, J.-P. Sauvage, C. O. Dietrich-Buchecker and J.-M. Kern, *J. Chem. Soc. Faraday Trans.*, 1992, **88**, 553–556.

44 W. D. Horrocks, J. P. Bolender, W. D. Smith and R. M. Supkowski, *J. Am. Chem. Soc.*, 1997, **4**, 5972–5973.

45 S. Cotton, *Lanthanide and Actinide Chemistry*, 2005.

46 K. Binnemans, *Coord. Chem. Rev.*, 2015, **295**, 1–45.